Cancer Cell
Article

The Androgen Receptor Induces a Distinct Transcriptional Program in Castration-Resistant Prostate Cancer in Man

Naomi L. Sharma,[1,3,8,10] Charlie E. Massie,[1,8] Antonio Ramos-Montoya,[1] Vincent Zecchini,[1] Helen E. Scott,[1] Alastair D. Lamb,[1,3] Stewart MacArthur,[2] Rory Stark,[2] Anne Y. Warren,[4] Ian G. Mills,[1,6,7,8,9] and David E. Neal[1,3,5,8,*]
[1]Uro-oncology Research Group
[2]Department of Bioinformatics
Cambridge Research Institute, Cambridge, CB2 0RE, UK
[3]Department of Urology
[4]Department of Pathology
Addenbrooke's Hospital, Cambridge, CB2 2QQ, UK
[5]Department of Oncology, University of Cambridge, Cambridge, CB2 2QQ, UK
[6]Department of Urology
[7]Department of Cancer Prevention
Oslo University Hospital, 0424 Oslo, Norway
[8]These authors contributed equally to this work
[9]Present address: Prostate Cancer Research Group, Nordic EMBL Partnership, Centre for Molecular Medicine Norway (NCMM), University of Oslo, 0316 Oslo, Norway
[10]Present address: Nuffield Department of Surgical Sciences, University of Oxford, Oxford OX3 9DU, UK
*Correspondence: den22@medschl.cam.ac.uk
http://dx.doi.org/10.1016/j.ccr.2012.11.010

SUMMARY

The androgen receptor (AR) regulates prostate cell growth in man, and prostate cancer is the commonest cancer in men in the UK. We present a comprehensive analysis of AR binding sites in human prostate cancer tissues, including castrate-resistant prostate cancer (CRPC). We identified thousands of AR binding sites in CRPC tissue, most of which were not identified in PC cell lines. Many adjacent genes showed AR regulation in xenografts but not in cultured LNCaPs, demonstrating an in-vivo-restricted set of AR-regulated genes. Functional studies support a model of altered signaling in vivo that directs AR binding. We identified a 16 gene signature that outperformed a larger in-vitro-derived signature in clinical data sets, showing the importance of persistent AR signaling in CRPC.

INTRODUCTION

Transcription factors (TFs) bind selectively to specific DNA sequences and regulate developmental and pathogenic transcriptional programs (Badis et al., 2009; Roche et al., 1992). However, interactions between TFs can have a dramatic effect on their genomic targeting, as in the case of FOXA1-dependent recruitment of the androgen receptor (AR) and estrogen receptor (ER) (Lupien et al., 2008) or STAT5-directed recruitment of the glucocorticoid receptor (Stoecklin et al., 1997) to specific targets. This interdependence and the diverse signals that affect TF activity support a dynamic, context-dependent model for their genomic targeting.

The study of oncogenic TFs has provided important mechanistic insights into cancer biology (Hurtado et al., 2008; Palomero et al., 2006; Wei et al., 2006). The AR is the main target of hormonal therapies used in prostate cancer (PC), but despite initial response to therapy, a large proportion of patients develop

Significance

This study confirms the importance of the AR in CRPC and shows that cellular context is important in the functional genomic positioning of the AR. It demonstrates a tissue-specific transcriptional network not observed in cultured cells, with specific implications for our understanding and management of CRPC. The core 16 gene set identified in this study, which would otherwise not have been implicated in CRPC, has revealed potential targets for therapeutic intervention and monitoring of disease progression. This highlights the wider need to utilize clinical material for the study of oncogenic transcription factors by demonstrating the critical role of cellular context in the regulation of transcription factor target selection and gene regulation.

castrate-resistant PC (CRPC), which leads to death in 12–24 months. Many studies have described in detail the transcriptional programs and pathways downstream of the AR, but the authors used cultured cells with only selected ARBS tested in tissue (Massie et al., 2011; Wang et al., 2009; Yu et al., 2010). Application of these in-vitro-derived AR signatures to tissue-expression profiles suggested a loss of AR signaling in CRPC (Tomlins et al., 2007; Yu et al., 2010), a finding at odds with both observations from functional studies (Chen et al., 2004; Snoek et al., 2009) and the success of novel therapies targeting AR signaling in CRPC (Attar et al., 2009; Attard et al., 2008; Tran et al., 2009), suggesting that cell lines may not always accurately model the AR transcriptional program in human tumors.

RESULTS

We mapped the genome-wide occupancy of the AR in prostate tissue of 12 patients using chromatin immunoprecicpitation sequencing (ChIP-seq). Samples were rich in epithelium (mean 67%), with the exception of androgen-deprivation treatment-responsive (TR) samples, which were almost exclusively stromal. AR expression was medium-high intensity in 9/10 PC samples, but was absent or low in benign prostatic hyperplasia, and was epithelial in all except for the TR samples (Table S1 and Figure S1 available online).

ARBS Can Be Identified in Human Prostate Tissue

AR-ChIP DNA was validated by assessing enrichment at known AR binding sites (Figure 1A). Genome-wide AR-occupied regions in 12 tissue samples were identified using ChIP-seq with thousands of ARBS in human tissue (4,000 in at least two samples), including established AR targets such as the *KLK3* and *TMPRSS2* enhancers (Figures 1A, 1B, and 1D). Pairwise comparisons of AR binding profiles for tissue samples and three unrelated PC cell lines (LNCaP, VCaP, 22RV1) highlighted two clusters, reflecting (1) ARBS found predominantly in benign and untreated PC tissue and (2) ARBS found in CRPC tissue and cell lines (Massie et al., 2011) (Figure 1C). Benign samples had significantly fewer ARBS than did CRPC samples ($p < 0.02$), which may reflect their lower levels of AR expression (Table S1). TR samples also yielded low numbers of ARBS and were the most divergent from the other AR binding profiles, reflecting stromal AR expression and absence of prostate epithelium (Table S1). The highest correlations were between the different PC cell lines, possibly reflecting their identical growth conditions (Figure 1C). All commercially available cell lines that have previously been characterized by AR ChIP-seq are derived from metastatic deposits of PC and therefore might not accurately reflect AR activity in primary PC, as there is substantial evidence for altered expression profiles of androgen-regulated genes in metastatic versus primary PC (Glinsky et al., 2004; Tomlins et al., 2007; Varambally et al., 2005; Yu et al., 2004). Comparisons of ARBS identified in untreated and CRPC tissue with those in cultured PC cell lines revealed that these models were indeed most similar to CRPC tissue (31% overlap, Table S2). Importantly, ARBS identified in untreated and CRPC tissue overlapped by 30% (Table S2), while there was only a 3% overlap between the ARBS in untreated PC tissue and cell lines (Table S2). This highlights a common subset of AR target genes between untreated PC and CRPC and identifies a divergence in AR binding profiles between cultured cells and primary tissue.

A Unique AR Transcriptional Program Exists in PC Tissue

Over 50% of ARBS identified in CRPC tissue were not found in PC cell lines but were highly conserved and represented tissue-specific sites, such as *EIF2B5* (Figures 1E, 1F, and 2A). Binding sites of histone marks H3K4me1 and H3K4me3 are often used to classify sites that are associated with active transcription from the rest of the sites in whole-genome TF data sets; therefore, ChIP-seq of these marks was undertaken in an additional two CRPC tissue samples. ChIP-seq of histone marks H3K4me1 and H3K4me3 in CRPC tissue revealed overlapping binding sites with the AR (26.2% of the AR peaks overlap with H3K4 peaks in CRPC tissue; 0.81% of H3K4 peaks overlap with AR peaks in CRPC tissue). The overlap between histone-mark peaks and AR peaks was much lower in TR/untreated tissue samples (17% and 4% for H3K4me1 and H3K4me3, respectively) and with the AR in cultured cells (11% and 1% for H3K4me1 and H3K4me3, respectively). The majority of genes that show AR binding in CRPC tissue also have H3K4me1/me3 peaks (95% and 89%, respectively), further supporting the activation of these AR target genes in vivo (Figures 1D and 1E). Enrichment of H3K4me1 binding was identified at enhancers and enrichment of H3K4me3 binding was identified at promoters in all tissue samples (benign prostate tissue, TR PC, and CRPC tissue) and was consistent with previous studies (Wang et al., 2011; Yu et al., 2010) (Figures 2B and 2C).

Many of the genes adjacent to ARBS in CRPC tissue showed androgen-regulated expression in cultured LNCaP cells (Figure 3A), with preferential co-occurrence of the AR and H3K4me3 observed at promoters of AR-regulated genes (observed overlaps of 24% and 6% at AR-regulated genes and AR-regulated gene promoters, compared to expected overlaps of 5% and 2%, respectively, $p = 2.99 \times 10^{-32}$ and $p = 2.23 \times 10^{-6}$). However, 44% of genes adjacent to CRPC ARBS showed no evidence of AR regulation in LNCaP PC cell culture conditions (Figure 3A). Importantly, the majority of these CRPC tissue AR targets were differentially regulated in LNCaP xenografts following castration, including over one-third of genes that had shown no androgen regulation in vitro (Figure 3B). The in vivo regulation of these genes by the AR was further demonstrated by differential expression in clinical samples from patients with PC who were receiving neoadjuvant hormone treatment (Figure 3C), in an unrelated xenograft model (Figure 4A), and in clinical samples from patients with untreated PC and CRPC in two separate studies (Figures 4B and 4C).

In order to directly compare the in vitro and in vivo androgen regulation of the AR bound genes identified in CRPC tissue, we visualized gene-expression changes using two-dimensional density plots (Shu et al., 2003; Venables and Ripley, 2002). Genes bound by the AR in vitro (cell line ARBS within 25 kb) had a strong shift toward androgen upregulation in vitro and also evidence of downregulation in response to castration in PC xenografts (Figure 4D). In contrast, genes bound by the AR in vivo (CRPC tissue ARBS within 25 kb) showed an equally strong in vivo response to castration but a markedly lesser response to in vitro androgen stimulation (Figure 4D). This

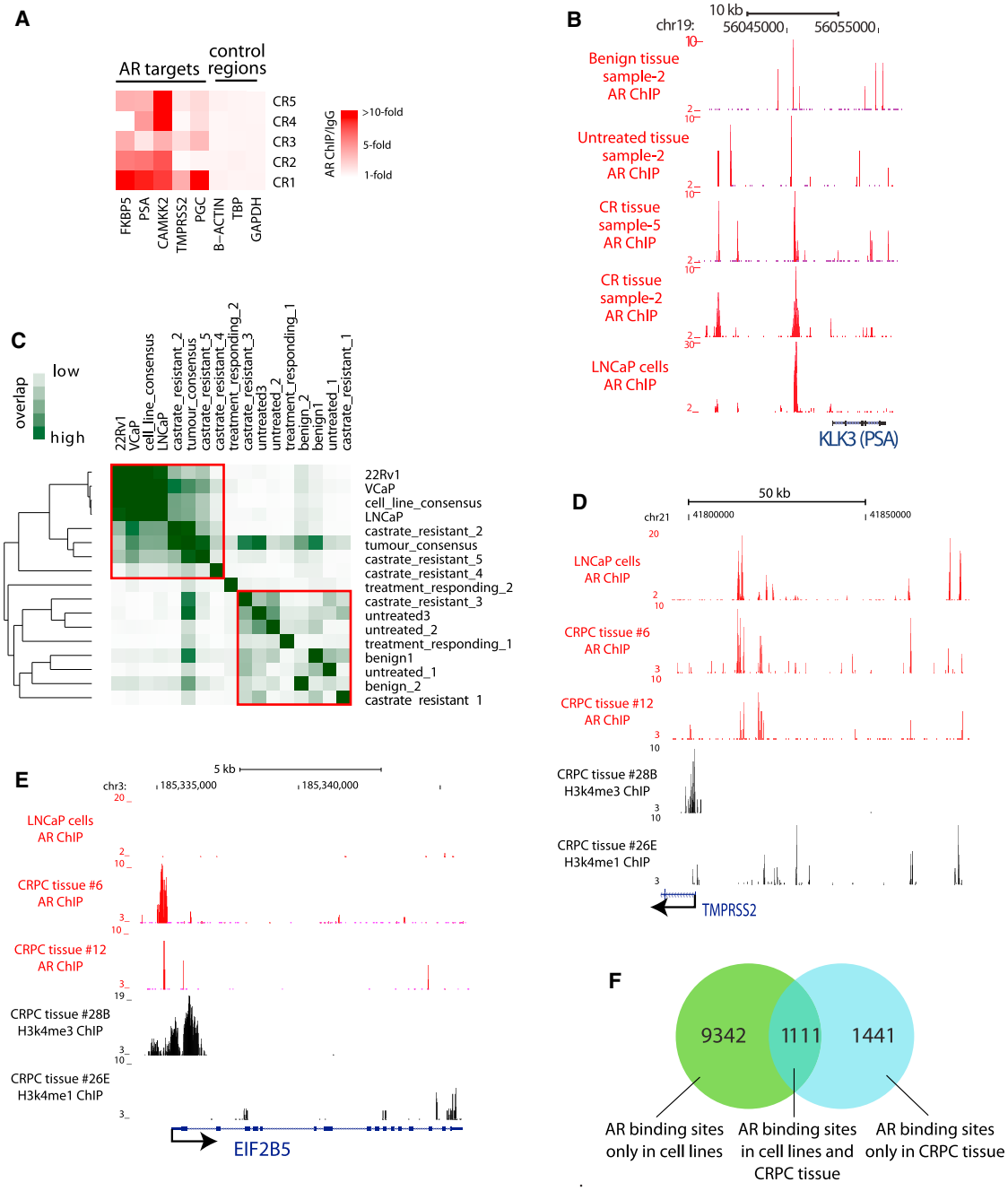

Figure 1. AR Binding Sites Mapped in Prostate Cancer Tissue Identify Divergent AR Binding Profiles In Vivo

(A) ChIP-PCR validation of known AR-regulated genes in CRPC-tissue AR ChIP, enrichment normalized to IgG control and relative to housekeeping genes b-actin, GAPDH, and TBP.

(B) AR ChIP-seq enrichment profiles for benign, untreated prostate cancer (PC), castrate-resistant (CR) PC tissue, and LNCaP cells at the *KLK3* (*PSA*) locus.

(C) Heatmap showing the concordance between AR ChIP sets from each tissue sample, cell line, and consensus binding sites (represented as percentage of set, main subclusters highlighted by red boxes).

(D) Example of concordant binding in LNCaP cells and CRPC tissue of the AR and histone marks at the *TMPRSS2* locus.

(E) Example of CRPC tissue AR binding and histone marks that were not found in cell lines at the *EIF2B5* locus.

(F) Venn diagram showing the pairwise overlap between AR binding sites identified in cell lines (VCaP and LNCaP) and those in CRPC tissue.

See also Table S1 and Figure S1.

in-vivo-restricted androgen regulation was highlighted in the subset of AR targets identified in CRPC tissue that showed no evidence of in vitro androgen regulation, where there was clear downregulation in response to castration of PC xenografts (Figure 4D). Gene-expression changes in primary PC tumors treated with neoadjuvant hormone therapy (NHT, chemical castration;

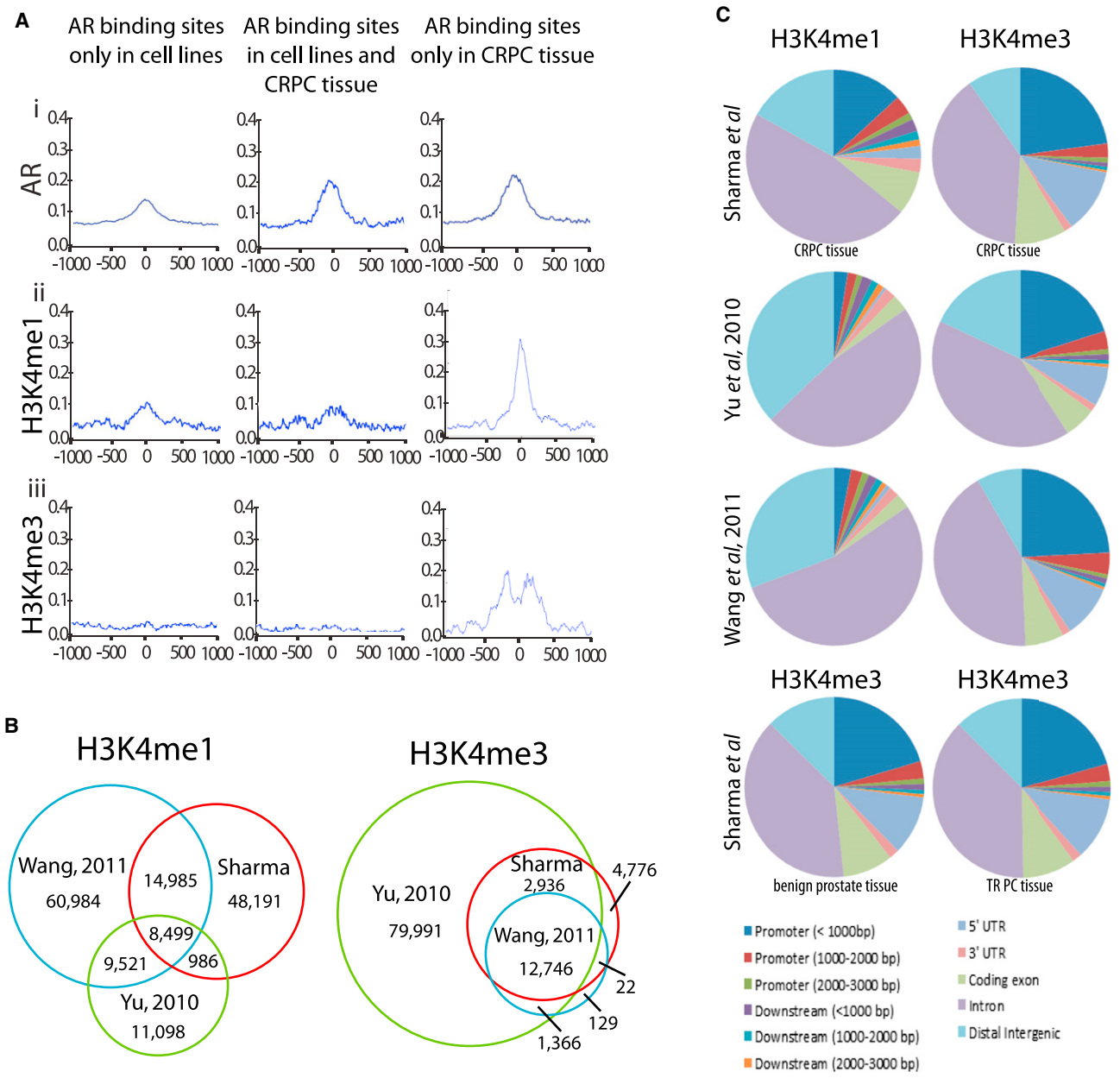

Figure 2. AR Binding Sites and Active Regulatory Elements Mapped in PC Tissue

(A) Average conservation plots of binding sites identified only in cell lines, only in CRPC tissue, and in both cell lines and CRPC tissue, for the AR, AR/H3K4me1 overlapping sites, and AR/H3K4me3 overlapping sites, using CEAS (Ji et al., 2006).

(B) Venn diagram showing overlap of H3K4me1/3 peaks from CRPC tissue in this study with those observed by Yu et al., 2010 and Wang et al., 2011.

(C) CEAS genomic analysis of histone mark binding sites identified in benign, TR (treatment-responding) PC, and CRPC tissue in this and other studies (Yu et al., 2010; Wang et al., 2011).

See also Table S2.

Mostaghel et al., 2007) revealed that genes bound by the AR in cultured PC cell lines showed little in vivo response to androgen withdrawal (Figure 4E). However, AR targets identified in CRPC tissue showed stronger gene-expression changes in response to NHT therapy, further highlighted in the subset of genes that showed no evidence of in vitro regulation (Figure 4E). Together these data provide clear evidence for a subset of in-vivo-restricted AR-regulated genes, supporting our identification of functional AR targets in PC tissue and highlighting the divergence from AR targets identified in cultured cells.

Divergent Transcriptional Complexes Are Present at ARBS In Vitro and In Vivo

Genomic analysis of AR binding sites in CRPC tissue identified higher enrichment at promoters compared to binding sites in cell lines and in untreated PC tissue (Figure 5A), with untreated

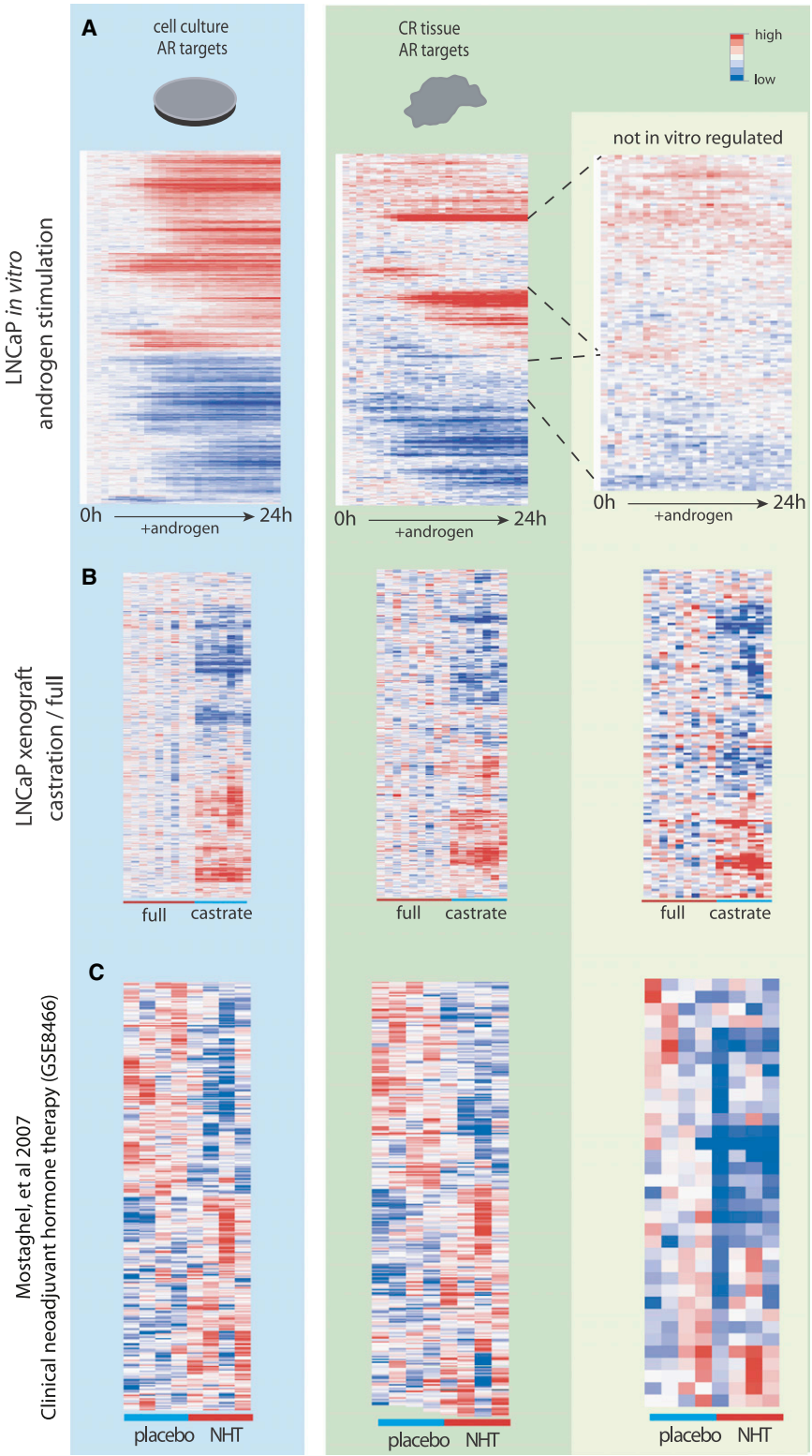

Figure 3. AR Targets Identified in CRPC Tissue Reveal In Vivo AR-Regulated Genes

(A) Gene-expression heatmaps showing LNCaP in vitro androgen stimulation profiles of candidate AR target genes identified in cell lines or CRPC tissue (genes <25 kb from AR binding sites, GSE18684). Subset of CRPC tissue AR targets not androgen-regulated in vitro are plotted separately (right).

(B) Gene expression heatmap from LNCaP PC xenograft models from tumors in full and castrated mice (unpublished data), subset as in (A).

(C) Gene-expression heatmap from a clinical trial of neoadjuvant hormone therapy (NHT, acyline) versus placebo (Mostaghel et al., 2007), subset as in (A).

PC tissue showing a shift toward higher intergenic binding, as was seen in CRPC tissue, suggesting that the AR binding profile in PC changes with disease progression. Motif analysis of the ARBS identified in benign prostate tissue identified AR binding motifs as the only significantly enriched motif, while in untreated PC the most enriched motifs included those for the AR, forkhead, and NF1 TFs (Table S3). GREAT analysis (McLean et al., 2010) revealed that ARBS in untreated PC tissue were enriched for genes involved in Notch, MAPK, and calcium signaling and aerobic respiration. These were not enriched among benign ARBS, possibly reflecting signaling and metabolic changes in the progression to PC. ARBS found in PC tissue were also enriched for genes associated with metabolic stress (increased cholesterol and increased body fat), whereas ARBS from cultured cells were most highly enriched for in vitro stimulation with androgens and forskolin (Figure 5B). Genes upregulated in PC samples and specific sets of metabolic genes were enriched only near ARBS found in CRPC tissue, suggesting a divergent transcriptional program regulated by the AR in CRPC tissue (Figure 5B).

Motif analysis of the genomic sequences underlying ARBS revealed significant enrichment of consensus AR binding motifs in both CRPC and cell lines (Figure 6A; Table S3). However, AR binding sites identified only in CRPC tissue were enriched for E2F, MYC, and STAT motifs (as were AR-H3K4me1/3 marked regions) but not for AR-associated TFs FOXA1 and NF-1, as previously defined in tissue culture (Gao et al., 2003; Jia et al., 2008) (Figures 6A and 6B). Comparisons of cell-line and tissue ARBS with publicly available TF ChIP-seq data sets (Consortium, 2011) showed that ARBS identified in tissue overlapped with E2F, MYC, STAT, NFKB, YY1, and GATA binding sites, while ARBS in cell lines showed no enrichment for these (Figure 6C). Additionally, genes associated with

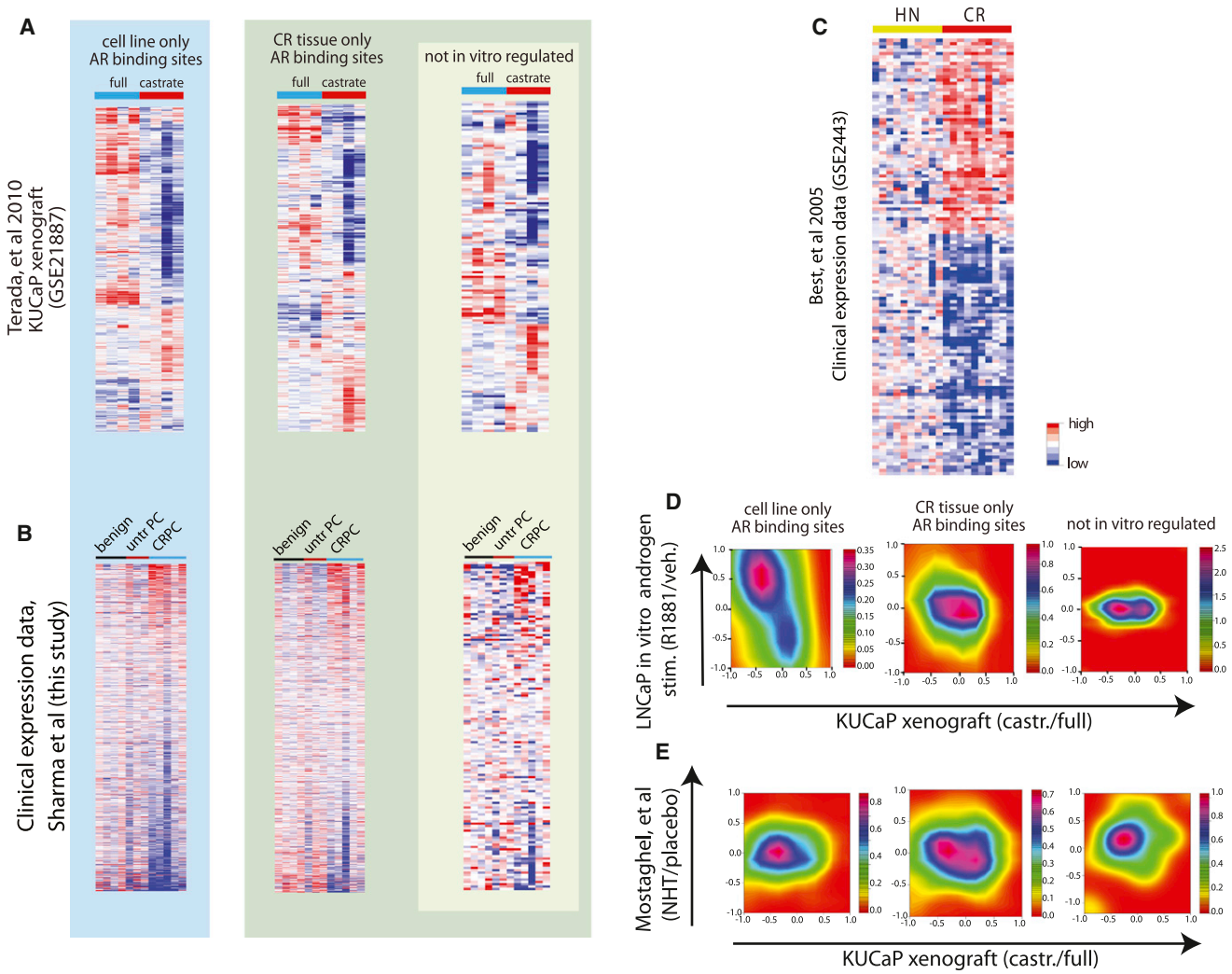

Figure 4. Surgical and Chemical Castration Regulate AR Target Genes Identified in PC Tissue

(A) Gene-expression heatmaps from KUCaP (Terada et al., 2010) PC xenograft models from tumors in full and castrated mice, subset by AR targets identified in cell lines, AR targets identified in CRPC tissue, and those AR targets identified in tissue that are not AR-regulated in vitro.

(B) Gene-expression heatmaps showing human prostate tissue (benign, untreated, or CRPC) profiles of candidate AR targets identified in cell lines or CRPC tissue.

(C) Gene-expression heatmap from hormone naive (HN) PC and CRPC (Best et al., 2005) showing AR target genes identified in CRPC tissue.

(D) Gene-expression changes in cultured LNCaPs treated with androgens (GSE18684) and KUCaP xenografts following castration (GSE21887) and NHT-treated PC tumors (GSE8466), represented as two-dimensional density plots. Color changes represent the density of genes with a given expression pattern over the two dimensions (as indicated on color scales), grouped as in (A).

(E) Gene-expression changes in NHT-treated PC tumors and KUCaP xenografts following castration represented as two-dimensional density plots, grouped as in (A).

ARBS in PC tissue (<25 kb distant) were significantly enriched ($p < 0.05$, FDR ≤ 0.25) for genes regulated by MYC, E2F, and IL6 (an activator of JAK/STAT) (Figure 6F).

To determine whether cellular context may contribute to the observed change in AR binding profile between cultured cells and CRPC tissue, we assessed AR interacting proteins in cultured and xenografted LNCaP cells. This isogenic comparison revealed an attenuated AR-FOXA1 interaction in xenografts, in comparison with cultured cells, and also a gain of AR-STAT5 interaction in xenografts (Figures 6D and 6E). In addition, AR binding could be redirected to sites only occupied by the AR in PC tissue by treating cultured LNCaP cells with a cocktail of cytokines, which have previously been implicated in PC (Figure 6G; see Supplemental Experimental Procedures for details). We observed a clear increase in AR binding at 5/10 sites ($p < 0.05$) and a trend toward increased binding at a further 3/10 sites tested (Figure 6G). Together these data provide functional validation of the altered AR binding profile observed in CRPC tissue and provide insights into the molecular mechanisms that may underlie these changes.

A Clinically Relevant Signature Is Identified from PC Tissue

We next sought to test the utility of our PC tissue AR gene sets as markers of function in vivo and as markers of CRPC and prognosis. We identified a set of 150 AR target genes in CRPC tissue

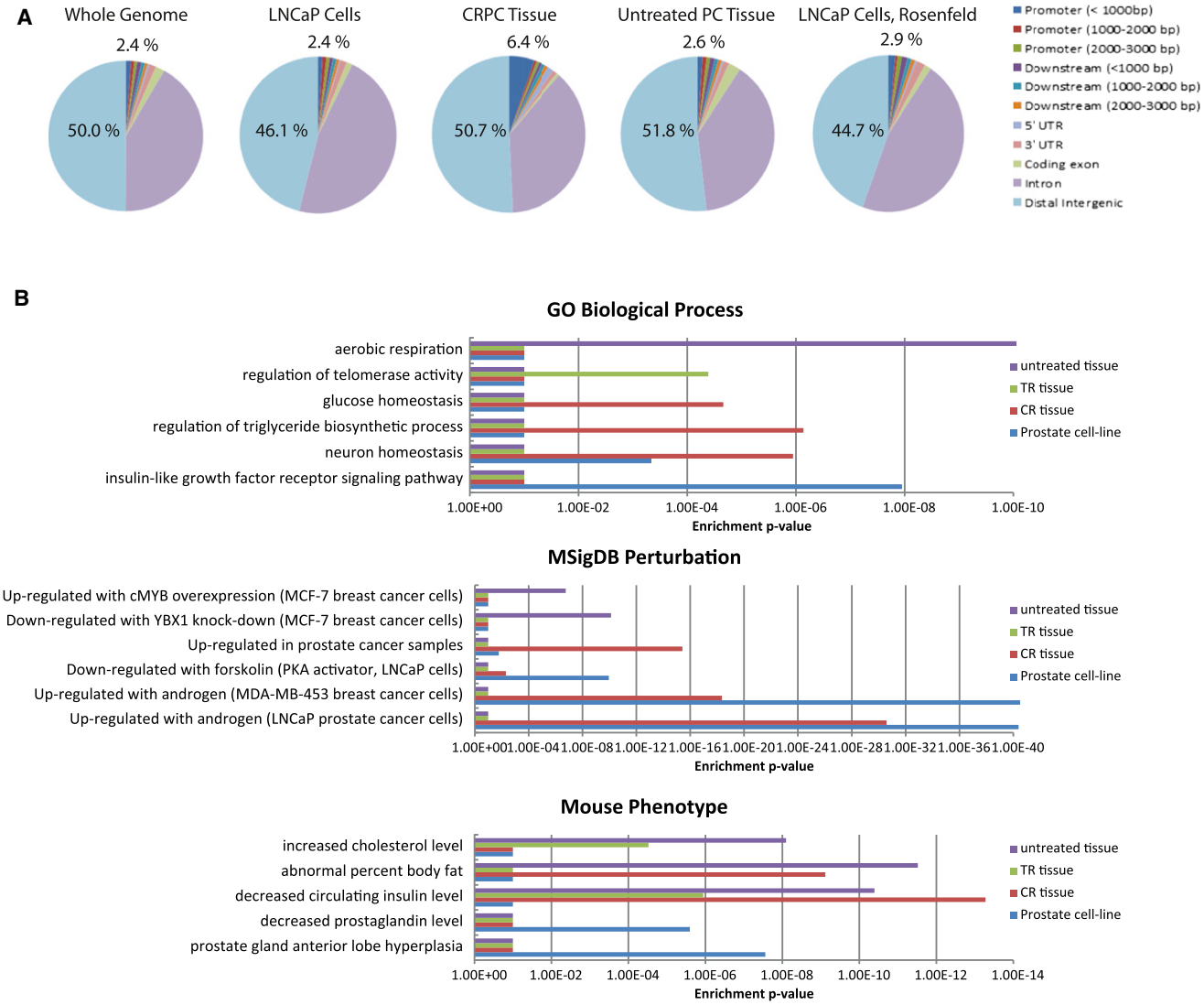

Figure 5. Distinct Transcriptional Targets of the AR and Downstream Signaling Pathways In Vitro and In Vivo

(A) Genomic location analysis of AR binding sites in LNCaP cell lines and CRPC and untreated PC tissue in comparison to the whole genome.

(B) GREAT (Genomic Regions Enrichment of Annotations Tool) analysis of AR binding sites identified in human tissue and cell lines, showing selected terms that passed significance for one or more sets of AR binding sites.

that were downregulated by castration in PC xenografts and were upregulated in CRPC tissue compared to untreated PC (Figures 7A and 7B; Table S4). Gene-set enrichment of these core 150 genes identified many of the same pathways as the full set of AR targets in CRPC tissue (Table S4). Selection of the genes with the most consistent changes across castrated xenografts and CRPC identified a core 16 gene signature (Table S4). All of these genes had increased expression in human CRPC tissue (Figure 7C) and all were downregulated by castration in xenografts, with the reemergence of a subset in CRPC xenografts (Figure 7D). This core set of 16 AR target genes in CRPC was enriched for E2F, STAT, and MYC binding sites (Consortium, 2011) (Figure 7F), consistent with the full set of CRPC AR binding sites (Figure 6). Gene-set analysis and direct comparison of gene-expression changes showed that this core 16 gene set had high gene-set enrichment scores for both in vitro AR-regulated genes and xenograft castration-regulated genes, similar to a published 250 gene "AR activity signature" (Mendiratta et al., 2009) (Figure 7E), but overall showed a stronger correlation with AR regulation in vivo (Figures 7E–7H; Figure S2). The core CRPC AR signature also showed strong gene-set enrichment for genes associated with CRPC and recurrent disease ($p < 0.05$ and FDR ≤ 0.25, Figure 7E), together with overall upregulation in CRPC tissue (Figure 7G), whereas the previously published signature showed little enrichment (Figure 7E) and no evidence of upregulation in CRPC (Figure 7G). These results were supported by an orthologous analysis using multidimensional scaling, which showed that the published AR gene signature (Mendiratta et al., 2009) captured more of the variance from in vitro AR stimulation, whereas our core CRPC tissue 16 gene

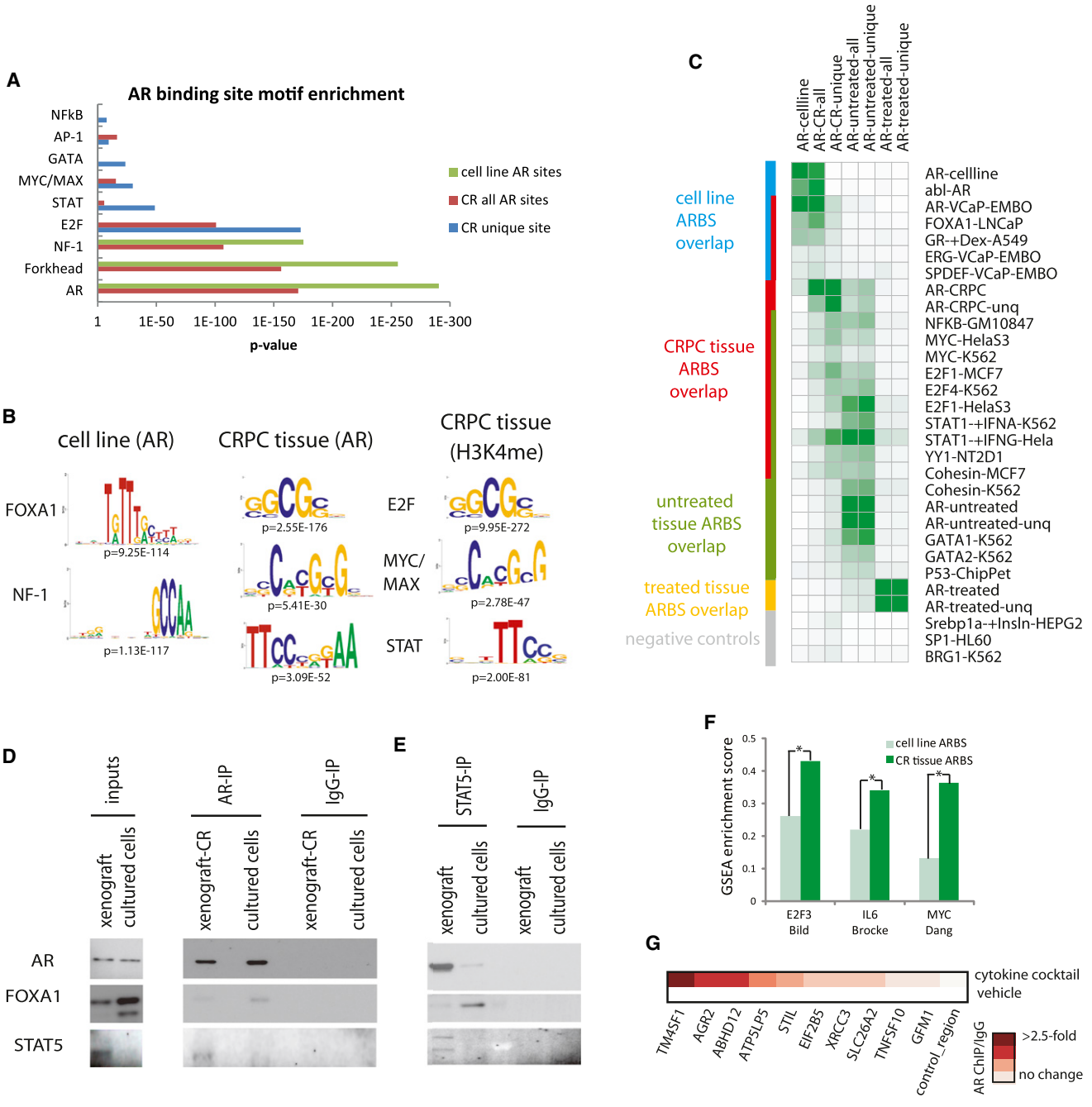

Figure 6. Divergent Transcriptional Complexes at AR Binding Sites In Vitro and In Vivo

(A) CEAS motif enrichment analysis of AR binding sites identified using ChIP-seq in PC cell lines (LNCaP and VCaP, Massie et al., 2011) and CR PC tissue.

(B) Sequence logos of transcription factor binding motifs enriched in cell line and CRPC tissue AR and histone-mark binding sites with enrichment p values, generated in CEAS.

(C) Heatmap showing the cell-line and tissue AR target set overlap with publicly available ChIP data for other transcription factors (Consortium, 2011) (expressed as % of set, annotated as "factor-cell line").

(D and E) AR immunoprecipitation (D) and STAT5 immunoprecipitation (E) in cultured and xenografted LNCaP PC cells, western blots of AR, FOXA1, and STAT5. IgG controls and inputs are shown for each immunoprecipitation sequence.

(F) Gene-set enrichment analysis (GSEA) using genes within 25 kb of AR binding sites identified in either cell lines or CRPC tissue; *$p < 0.05$.

(G) Heatmap showing AR ChIP enrichment of CRPC tissue-specific AR targets following treatment of LNCaP cells with cytokine cocktail (see Supplemental Experimental Procedures for details), enrichment normalized to IgG control and relative to housekeeping genes β-actin, GAPDH, and TBP.

See also Table S3.

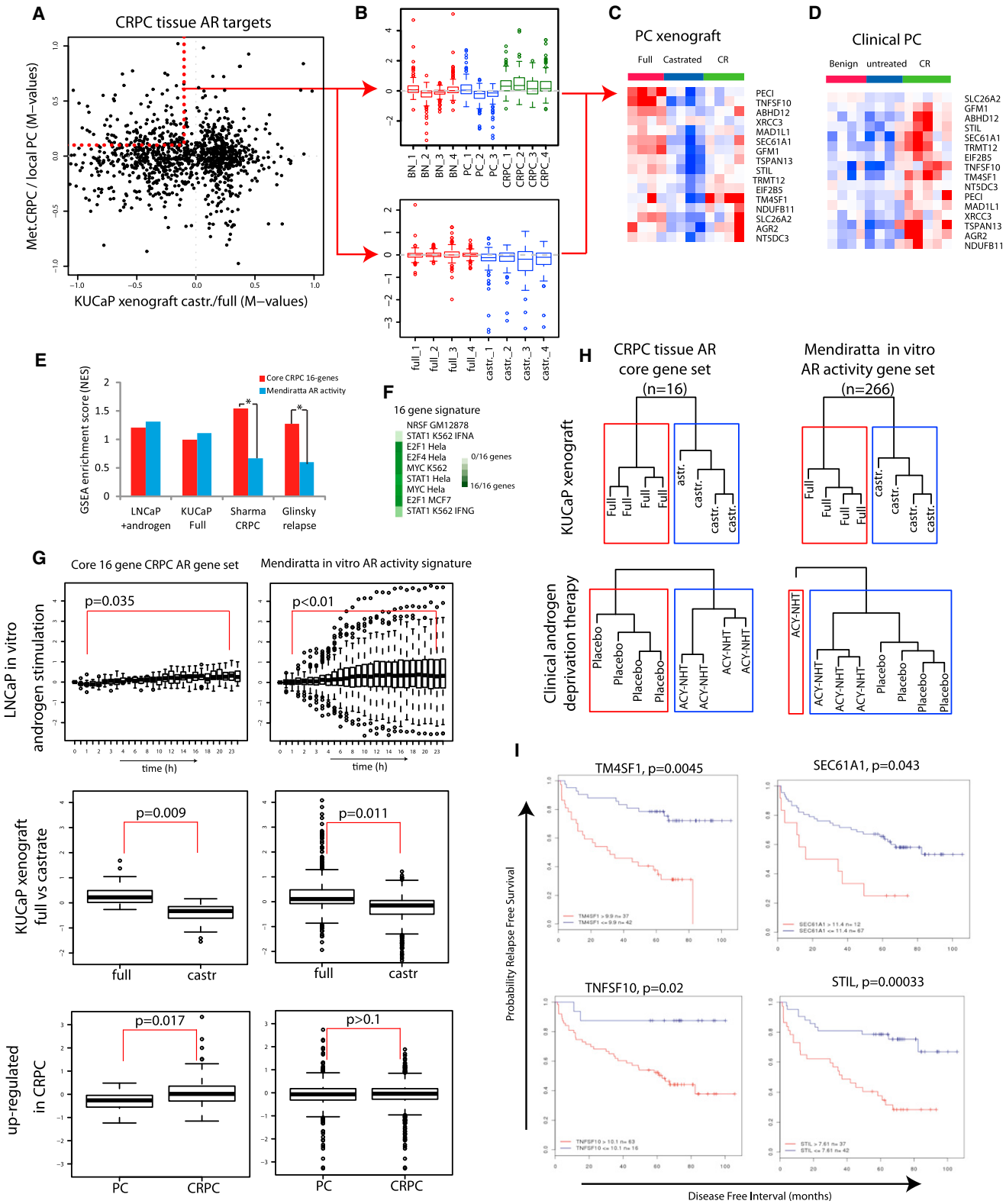

Figure 7. AR Signaling Is Maintained in Castrate-Resistant Prostate Cancer Tissue via a Distinct Set of AR Targets

(A) Scatter plot showing gene-expression changes of CRPC AR target genes in KUCaP xenografts (castrate/full) and clinical PC tissue (CRPC/PC) gene-expression data (log fold change, M-values). Red-outlined rectangle denotes 150 genes down following castration and up in CRPC.

(B) Box plots for 150 selected genes using gene-expression data from clinical PC tissue and KUCaP xenografts.

(legend continued on next page)

set performed better in both xenografts and PC tissue data sets (Figure S2). This core set of CRPC AR targets was also sufficient to faithfully segregate castrated from full PC xenografts and hormone-therapy-treated PC from placebo-treated PC (Figure 7H). In addition, genes from this 16 gene set were able to predict survival in two independent clinical data sets of PC (Glinsky et al., 2004, Taylor et al., 2010) (examples shown in Figure 7I).

We validated at the protein level a gene from this core signature, the tRNA methyltransferase *TRMT12*, which showed strong binding by the AR in CRPC tissue (Figure 8A) and exhibited in-vivo-restricted AR regulation (Figures 8B and 8C). TRMT12 transcript was also upregulated in CRPC tissue (Figure 8D). Immunohistochemistry revealed increased protein expression in CRPC tissue compared to benign and untreated or TR PC tissue both in samples taken from patients that were used for AR ChIP-seq and in a separate cohort of patients (Figure 8E).

DISCUSSION

This study has successfully demonstrated a comprehensive analysis of ARBS in a panel of human prostate tissue samples. Combined analysis identified ARBS in untreated PC that were lost in TR samples, a proportion of which were regained with the emergence of CR disease. Integration of AR binding profiles from cultured cells suggests that these models may more closely reflect CR disease, in keeping with their metastatic origins. Importantly, our combined analysis using prostate tissue identified a large number of ARBS not found in previous cell-line-based studies.

AR targets identified in CRPC tissue allowed us to address the apparently conflicting data on AR activity in CRPC. Using an isogenic system we were able to identify in vitro and in vivo AR-regulated genes, supporting direct AR regulation of the CRPC tissue-specific AR targets. Further validation of these targets using comparisons with an unrelated prostate cancer xenograft model (Terada et al., 2010) and clinical gene-expression data from patients treated with neoadjuvant hormone therapy provides evidence that the AR transcriptional program in tissue is divergent from that in cultured cells. The ARBS identified in tissue correlated much better with clinical gene-expression data sets than did the ARBS from cell lines, suggesting that tissue-derived data sets may more accurately reflect the in vivo targets of the AR in PC patients.

The tissue-specific ARBS identified in CRPC, as compared to cultured cells, are associated with in vivo androgen-regulated genes and converge with distinct transcription factor networks. This difference in AR activity between cultured cells and primary human tissue could be explained by genetic or epigenetic alterations in regulators of AR cooperating transcription factors (e.g., FOXA1 mutations, RB inactivation, DAB2IP downregulation) or by the integration of paracrine signaling events on other transcription factors to modulate AR activity (Figures 8F and 8G). Our functional studies in an isogenic system highlight the role of altered signaling (Figures 6D and 6G), suggesting that differential expression and activation of AR-interacting transcription factors contribute to the altered AR binding profile observed in human PC tissue.

Overlapping binding sites of the AR and histone marks in CRPC tissue and also the 16 gene signature we identified were strongly enriched for STAT, MYC, and E2F binding sites (Figures 6C and 7F), supporting the importance of these pathways in the progression and development of CRPC in man (Bernard et al., 2003; Ellwood-Yen et al., 2003; Gao et al., 2009; Hedvat et al., 2009; Sharma et al., 2010). We have demonstrated genomic repositioning of the AR in PC cells following treatment with a cytokine cocktail that stimulates these critical pathways. We have demonstrated in vitro versus in vivo changes in AR-interacting proteins, which confirm our computational analysis and provide a mechanistic explanation for the divergent AR binding profiles seen in CRPC tissue compared to cultured cells. Our preliminary functional studies highlight cellular context and altered cell signaling as one possible mechanism and highlight the need for detailed future studies to validate these pathways and to carefully address the transcription factor interplay in CRPC in vivo.

The divergent pathways identified in PC tissue and cultured cells, supported by xenograft data, highlight a distinct transcriptional program downstream of the AR targets in CRPC tissue, wherein AR signaling regulates cellular processes that contribute to both oncogenic and stem cell potential (e.g., proliferation, metabolism, steroid biosynthesis).

The 16 gene signature identified in this study was better able to predict CRPC and recurrent PC than a larger published AR signature, supporting the use in future TF studies of clinical samples to determine clinically relevant information. This signature also highlights the utility of these targets as potential markers of progression and response to therapy in CRPC, with a subset of genes (including *TNFSF10* and *TM4SF1*) significantly predictive of survival in two independent clinical expression data sets (Glinsky et al., 2004; Taylor et al., 2007). These gene sets may be particularly useful in monitoring the efficacy of second-generation agents targeting AR signaling when classical markers such as prostate-specific antigen are lost.

(C) Gene-expression heatmap showing LNCaP xenograft castration profiles of the core 16 AR CRPC gene set.
(D) Gene-expression heatmap showing segregation of CRPC samples from benign and untreated hormone-naive PC samples (GSE28680) using the core 16 AR target gene set identified in CRPC tissue.
(E) GSEA enrichment scores for genes in either the core 16 gene AR CRPC set or a larger in-vitro-derived AR activity signature (Mendiratta et al., 2009) using expression data from in vitro AR activation (GSE18684), xenograft castration (GSE21887), CRPC (GSE2443), and recurrent PC genes (Glinsky et al., 2004); $^{*}p < 0.05$.
(F) Heatmap showing enrichment of core 16-gene signature in publicly-available transcription factor ChIP data sets (Consortium, 2011).
(G) Box plots showing gene expression changes from in vitro androgen stimulation (GSE18684), xenograft castration (GSE21887)-regulated genes, and CRPC (GSE2443) using genes from our core 16 gene set or a published AR signature.
(H) Hierarchical clustering of castrated versus full xenografts and primary PC tumors treated with neoadjuvant hormone therapy (NHT-ACY) versus placebo. Clustering was performed using the subset of genes in our core 16 gene CRPC AR set and the published in vitro AR activity signature.
(I) Kaplan-Meier survival curves showing significant predictive ability of four core AR target genes, TM4SF1, SEC61A1, TNFSF10, and STIL (Glinsky et al., 2004).
See also Figure S2 and Table S4.

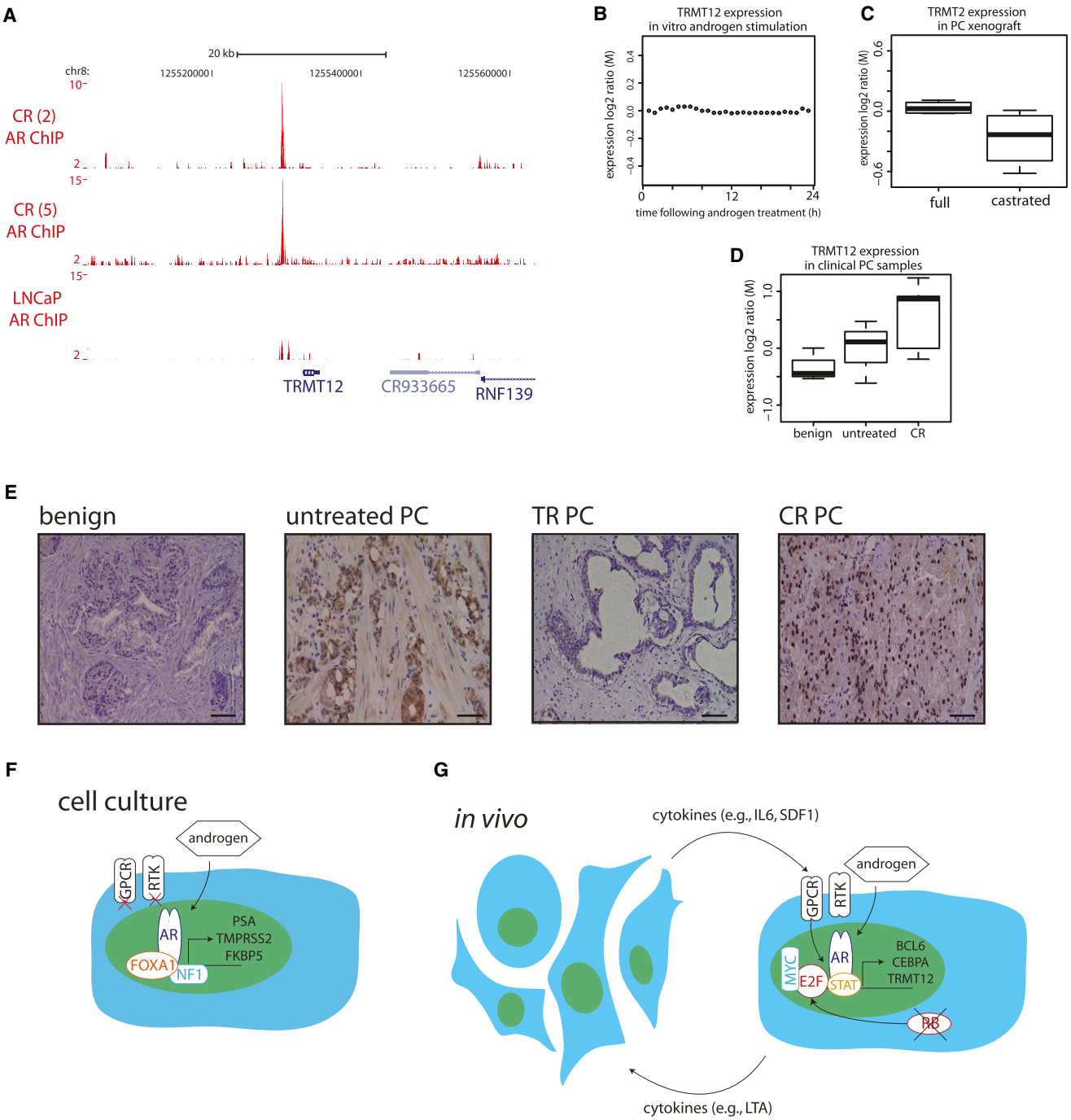

Figure 8. AR Signaling in Castrate-Resistant Prostate Cancer Tissue: Candidate Markers and Contributing Mechanism

(A) AR binding profile from cultured LNCaPs and CRPC tissue at the TRMT12 locus, as an example from the core 16 CRPC AR gene set.

(B) LNCaP in vitro androgen stimulation gene-expression profile for TRMT12.

(C) PC xenograft full and castrate gene expression of TRMT12.

(D) TRMT12 gene expression in clinical PC samples (benign, untreated, and castrate resistant).

(E) Immunohistochemistry for TRMT12 in benign and untreated, androgen-deprivation therapy-responding and castrate-resistant prostate cancer tissue (scale bar represents 200 microns).

(F and G) Schematic showing possible models of divergent targeting of the AR in vitro (F) and in vivo (G).

Our study provides insights into the pathways both up- and downstream of AR signaling in prostate cancer tissue and, importantly, has revealed functional and tissue-specific targets of the AR in human CRPC. We have identified potential targets for therapeutic intervention, particularly with respect to cell-cycle regulation and metabolism, and others

that could be used to monitor disease progression. Many of these tissue-specific AR targets are regulated by three other major classes of TF (STAT, c-Myc, and E2F families), which lie downstream of genetic alterations in PC (Sharma et al., 2010) and paracrine signaling pathways implicated in CRPC biology (Tam et al., 2007). Our study underscores the importance of cellular context in determining not only gene-expression patterns but also the binding profiles of specific TFs in the study of disease.

EXPERIMENTAL PROCEDURES

Clinical Samples

All clinical samples were collected from Cambridge University Hospitals NHS Trust as part of the ProMPT study, and ethical approval was granted by the local research and ethics committee (LREC number: 02/281M) and by the multicenter research and ethics committee (MREC number 01/4/061). Informed consent was obtained from all subjects. Fresh tissue was obtained at the time of transurethral resection of the prostate from ten patients with PC (five castrate-resistant [CR], two androgen-deprivation-therapy responsive [TR], and three untreated), and two men with benign prostate hyperplasia (Table S1).

ChIP and Gene Expression

ChIP was performed as previously described (Massie et al., 2007; Schmidt et al., 2008; Wilson et al., 2008), with enrichment tested by Realtime polymerase chain reaction using SYBRgreen (Applied Biosystems) (details in Supplemental Experimental Procedures). Single-end SOLEXA libraries were prepared as previously described (Schmidt et al., 2008), and 36 bp sequence reads were generated and analyzed (details in Supplemental Experimental Procedures). Details of RNA extraction and Illumina expression arrays are in Supplemental Experimental Procedures.

Data Analysis

ARBS identified in individual PC tissue samples and cell lines were compared by calculating the percentage overlap of BS ($\geq$1 bp overlap) for all pairwise comparisons between samples, correlated using Eisen Cluster (Eisen et al., 1998) and plotted as heatmaps. Overlap, subtraction, union, and feature annotation of ChIP-seq enriched regions were done using the Galaxy website (Blankenberg et al., 2007; Taylor et al., 2007). Motif-enrichment analysis and evolutionary conservation of the ARBS identified in cell lines and each tissue subtype were performed using CEAS (Ji et al., 2006). Functional annotation of the genes associated with each of the ARBS was performed using GREAT (McLean et al., 2010) and GSEA (Mootha et al., 2003; Subramanian et al., 2005). ARBS were integrated with gene expression data using a genomic window of 50 kb, and these genes were used to mine publicly available expression data sets (details in Supplemental Experimental Procedures). The core set of AR target genes in CRPC was identified by using t tests to rank genes within 25 kb genomic windows of ARBS for androgen-regulated expression (GSE18684) and expression in clinical PC samples (GSE28680).

Cell Assays

Western blotting (AR, FOXA1, and STAT5) and coimmunoprecipitations (AR and STAT5) were performed in LNCaP cells and xenografts (details in Supplemental Experimental Procedures).

Immunohistochemistry

Immunohistochemistry was performed using AR-N20 (Santa Cruz #sc-816) and TRMT12 (Atlas #HPA023939) antibodies at 1:100 dilution.

ACCESSION NUMBERS

All expression array data and ChIP-seq data generated in this study have been deposited in GEO (GSE28680 and GSE28219, respectively).

SUPPLEMENTAL INFORMATION

Supplemental Information includes two figures, four tables, and Supplemental Experimental Procedures and can be found with this article online at http://dx.doi.org/10.1016/j.ccr.2012.11.010.

ACKNOWLEDGMENTS

We are grateful to study volunteers for their participation and staff at the Welcome Trust Clinical Research Facility, Addenbrooke's Clinical Research Centre, Cambridge. We also thank the NIHR Cambridge Biomedical Research Centre, the DOH HTA (ProtecT grant), and the NCRI/MRC (ProMPT grant) for help with the bio-repository, and Cancer Research UK for funding.

Received: August 11, 2011
Revised: March 30, 2012
Accepted: November 19, 2012
Published: December 20, 2012

REFERENCES

Attar, R.M., Jure-Kunkel, M., Balog, A., Cvijic, M.E., Dell-John, J., Rizzo, C.A., Schweizer, L., Spires, T.E., Platero, J.S., Obermeier, M., et al. (2009). Discovery of BMS-641988, a novel and potent inhibitor of androgen receptor signaling for the treatment of prostate cancer. Cancer Res. *69*, 6522–6530.

Attard, G., Reid, A.H., Yap, T.A., Raynaud, F., Dowsett, M., Settatree, S., Barrett, M., Parker, C., Martins, V., Folkerd, E., et al. (2008). Phase I clinical trial of a selective inhibitor of CYP17, abiraterone acetate, confirms that castration-resistant prostate cancer commonly remains hormone driven. J. Clin. Oncol. *26*, 4563–4571.

Badis, G., Berger, M.F., Philippakis, A.A., Talukder, S., Gehrke, A.R., Jaeger, S.A., Chan, E.T., Metzler, G., Vedenko, A., Chen, X., et al. (2009). Diversity and complexity in DNA recognition by transcription factors. Science *324*, 1720–1723.

Bernard, D., Pourtier-Manzanedo, A., Gil, J., and Beach, D.H. (2003). Myc confers androgen-independent prostate cancer cell growth. J. Clin. Invest. *112*, 1724–1731.

Best, C.J., Gillespie, J.W., Yi, Y., Chandramouli, G.V., Perlmutter, M.A., Gathright, Y., Erickson, H.S., Georgevich, L., Tangrea, M.A., Duray, P.H., et al. (2005). Molecular alterations in primary prostate cancer after androgen ablation therapy. Clin. Cancer Res. *11*, 6823–6834.

Blankenberg, D., Taylor, J., Schenck, I., He, J., Zhang, Y., Ghent, M., Veeraraghavan, N., Albert, I., Miller, W., Makova, K.D., et al. (2007). A framework for collaborative analysis of ENCODE data: making large-scale analyses biologist-friendly. Genome Res. *17*, 960–964.

Chen, C.D., Welsbie, D.S., Tran, C., Baek, S.H., Chen, R., Vessella, R., Rosenfeld, M.G., and Sawyers, C.L. (2004). Molecular determinants of resistance to antiandrogen therapy. Nat. Med. *10*, 33–39.

Consortium, E.P.; ENCODE Project Consortium (2011). A user's guide to the encyclopedia of DNA elements (ENCODE). PLoS Biol. *9*, e1001046.

Eisen, M.B., Spellman, P.T., Brown, P.O., and Botstein, D. (1998). Cluster analysis and display of genome-wide expression patterns. Proc. Natl. Acad. Sci. USA *95*, 14863–14868.

Ellwood-Yen, K., Graeber, T.G., Wongvipat, J., Iruela-Arispe, M.L., Zhang, J., Matusik, R., Thomas, G.V., and Sawyers, C.L. (2003). Myc-driven murine prostate cancer shares molecular features with human prostate tumors. Cancer Cell *4*, 223–238.

Gao, N., Zhang, J., Rao, M.A., Case, T.C., Mirosevich, J., Wang, Y., Jin, R., Gupta, A., Rennie, P.S., and Matusik, R.J. (2003). The role of hepatocyte nuclear factor-3 alpha (Forkhead Box A1) and androgen receptor in transcriptional regulation of prostatic genes. Mol. Endocrinol. *17*, 1484–1507.

Gao, P., Tchernyshyov, I., Chang, T.C., Lee, Y.S., Kita, K., Ochi, T., Zeller, K.I., De Marzo, A.M., Van Eyk, J.E., Mendell, J.T., and Dang, C.V. (2009). c-Myc suppression of miR-23a/b enhances mitochondrial glutaminase expression and glutamine metabolism. Nature *458*, 762–765.

Glinsky, G.V., Glinskii, A.B., Stephenson, A.J., Hoffman, R.M., and Gerald, W.L. (2004). Gene expression profiling predicts clinical outcome of prostate cancer. J. Clin. Invest. *113*, 913–923.

Hedvat, M., Huszar, D., Herrmann, A., Gozgit, J.M., Schroeder, A., Sheehy, A., Buettner, R., Proia, D., Kowolik, C.M., Xin, H., et al. (2009). The JAK2 inhibitor AZD1480 potently blocks Stat3 signaling and oncogenesis in solid tumors. Cancer Cell *16*, 487–497.

Hurtado, A., Holmes, K.A., Geistlinger, T.R., Hutcheson, I.R., Nicholson, R.I., Brown, M., Jiang, J., Howat, W.J., Ali, S., and Carroll, J.S. (2008). Regulation of ERBB2 by oestrogen receptor-PAX2 determines response to tamoxifen. Nature *456*, 663–666.

Ji, X., Li, W., Song, J., Wei, L., and Liu, X.S. (2006). CEAS: cis-regulatory element annotation system. Nucleic Acids Res. *34*(Web Server issue), W551–W554.

Jia, L., Berman, B.P., Jariwala, U., Yan, X., Cogan, J.P., Walters, A., Chen, T., Buchanan, G., Frenkel, B., and Coetzee, G.A. (2008). Genomic androgen receptor-occupied regions with different functions, defined by histone acetylation, coregulators and transcriptional capacity. PLoS ONE *3*, e3645.

Lupien, M., Eeckhoute, J., Meyer, C.A., Wang, Q., Zhang, Y., Li, W., Carroll, J.S., Liu, X.S., and Brown, M. (2008). FoxA1 translates epigenetic signatures into enhancer-driven lineage-specific transcription. Cell *132*, 958–970.

Massie, C.E., Adryan, B., Barbosa-Morais, N.L., Lynch, A.G., Tran, M.G., Neal, D.E., and Mills, I.G. (2007). New androgen receptor genomic targets show an interaction with the ETS1 transcription factor. EMBO Rep. *8*, 871–878.

Massie, C.E., Lynch, A., Ramos-Montoya, A., Boren, J., Stark, R., Fazli, L., Warren, A., Scott, H., Madhu, B., Sharma, N., et al. (2011). The androgen receptor fuels prostate cancer by regulating central metabolism and biosynthesis. EMBO J. *30*, 2719–2733.

McLean, C.Y., Bristor, D., Hiller, M., Clarke, S.L., Schaar, B.T., Lowe, C.B., Wenger, A.M., and Bejerano, G. (2010). GREAT improves functional interpretation of *cis*-regulatory regions. Nat. Biotechnol. *28*, 495–501.

Mendiratta, P., Mostaghel, E., Guinney, J., Tewari, A.K., Porrello, A., Barry, W.T., Nelson, P.S., and Febbo, P.G. (2009). Genomic strategy for targeting therapy in castration-resistant prostate cancer. J. Clin. Oncol. *27*, 2022–2029.

Mootha, V.K., Lindgren, C.M., Eriksson, K.F., Subramanian, A., Sihag, S., Lehar, J., Puigserver, P., Carlsson, E., Ridderstråle, M., Laurila, E., et al. (2003). PGC-1α-responsive genes involved in oxidative phosphorylation are coordinately downregulated in human diabetes. Nat. Genet. *34*, 267–273.

Mostaghel, E.A., Page, S.T., Lin, D.W., Fazli, L., Coleman, I.M., True, L.D., Knudsen, B., Hess, D.L., Nelson, C.C., Matsumoto, A.M., et al. (2007). Intraprostatic androgens and androgen-regulated gene expression persist after testosterone suppression: therapeutic implications for castration-resistant prostate cancer. Cancer Res. *67*, 5033–5041.

Palomero, T., Lim, W.K., Odom, D.T., Sulis, M.L., Real, P.J., Margolin, A., Barnes, K.C., O'Neil, J., Neuberg, D., Weng, A.P., et al. (2006). NOTCH1 directly regulates c-MYC and activates a feed-forward-loop transcriptional network promoting leukemic cell growth. Proc. Natl. Acad. Sci. USA *103*, 18261–18266.

Roche, P.J., Hoare, S.A., and Parker, M.G. (1992). A consensus DNA-binding site for the androgen receptor. Mol. Endocrinol. *6*, 2229–2235.

Schmidt, D., Stark, R., Wilson, M.D., Brown, G.D., and Odom, D.T. (2008). Genome-scale validation of deep-sequencing libraries. PLoS ONE *3*, e3713.

Sharma, A., Yeow, W.S., Ertel, A., Coleman, I., Clegg, N., Thangavel, C., Morrissey, C., Zhang, X., Comstock, C.E., Witkiewicz, A.K., et al. (2010). The retinoblastoma tumor suppressor controls androgen signaling and human prostate cancer progression. J. Clin. Invest. *120*, 4478–4492.

Shu, G., Zeng, B., Chen, Y.P., and Smith, O.H. (2003). Performance assessment of kernel density clustering for gene expression profile data. Comp. Funct. Genomics *4*, 287–299.

Snoek, R., Cheng, H., Margiotti, K., Wafa, L.A., Wong, C.A., Wong, E.C., Fazli, L., Nelson, C.C., Gleave, M.E., and Rennie, P.S. (2009). In vivo knockdown of the androgen receptor results in growth inhibition and regression of well-established, castration-resistant prostate tumors. Clin. Cancer Res. *15*, 39–47.

Stoecklin, E., Wissler, M., Moriggl, R., and Groner, B. (1997). Specific DNA binding of Stat5, but not of glucocorticoid receptor, is required for their functional cooperation in the regulation of gene transcription. Mol. Cell. Biol. *17*, 6708–6716.

Subramanian, A., Tamayo, P., Mootha, V.K., Mukherjee, S., Ebert, B.L., Gillette, M.A., Paulovich, A., Pomeroy, S.L., Golub, T.R., Lander, E.S., and Mesirov, J.P. (2005). Gene set enrichment analysis: a knowledge-based approach for interpreting genome-wide expression profiles. Proc. Natl. Acad. Sci. USA *102*, 15545–15550.

Tam, L., McGlynn, L.M., Traynor, P., Mukherjee, R., Bartlett, J.M., and Edwards, J. (2007). Expression levels of the JAK/STAT pathway in the transition from hormone-sensitive to hormone-refractory prostate cancer. Br. J. Cancer *97*, 378–383.

Taylor, B.S., Schultz, N., Hieronymus, H., Gopalan, A., Xiao, Y., Carver, B.S., Arora, V.K., Kaushik, P., Cerami, E., Reva, B., et al. (2010). Integrative genomic profiling of human prostate cancer. Cancer Cell *18*, 11–22.

Taylor, J., Schenck, I., Blankenberg, D., and Nekrutenko, A. (2007). Using galaxy to perform large-scale interactive data analyses. Curr. Protoc. Bioinformatics (*Suppl 38*), 10.5.1–10.5.47.

Terada, N., Shimizu, Y., Kamba, T., Inoue, T., Maeno, A., Kobayashi, T., Nakamura, E., Kamoto, T., Kanaji, T., Maruyama, T., et al. (2010). Identification of EP4 as a potential target for the treatment of castration-resistant prostate cancer using a novel xenograft model. Cancer Res. *70*, 1606–1615.

Tomlins, S.A., Mehra, R., Rhodes, D.R., Cao, X., Wang, L., Dhanasekaran, S.M., Kalyana-Sundaram, S., Wei, J.T., Rubin, M.A., Pienta, K.J., et al. (2007). Integrative molecular concept modeling of prostate cancer progression. Nat. Genet. *39*, 41–51.

Tran, C., Ouk, S., Clegg, N.J., Chen, Y., Watson, P.A., Arora, V., Wongvipat, J., Smith-Jones, P.M., Yoo, D., Kwon, A., et al. (2009). Development of a second-generation antiandrogen for treatment of advanced prostate cancer. Science *324*, 787–790.

Varambally, S., Yu, J., Laxman, B., Rhodes, D.R., Mehra, R., Tomlins, S.A., Shah, R.B., Chandran, U., Monzon, F.A., Becich, M.J., et al. (2005). Integrative genomic and proteomic analysis of prostate cancer reveals signatures of metastatic progression. Cancer Cell *8*, 393–406.

Venables, W.N., and Ripley, B.D. (2002). Modern Applied Statistics with S, Fourth Edition (New York: Springer).

Wang, D., Garcia-Bassets, I., Benner, C., Li, W., Su, X., Zhou, Y., Qiu, J., Liu, W., Kaikkonen, M.U., Ohgi, K.A., et al. (2011). Reprogramming transcription by distinct classes of enhancers functionally defined by eRNA. Nature *474*, 390–394.

Wang, Q., Li, W., Zhang, Y., Yuan, X., Xu, K., Yu, J., Chen, Z., Beroukhim, R., Wang, H., Lupien, M., et al. (2009). Androgen receptor regulates a distinct transcription program in androgen-independent prostate cancer. Cell *138*, 245–256.

Wei, C.L., Wu, Q., Vega, V.B., Chiu, K.P., Ng, P., Zhang, T., Shahab, A., Yong, H.C., Fu, Y., Weng, Z., et al. (2006). A global map of p53 transcription-factor binding sites in the human genome. Cell *124*, 207–219.

Wilson, M.D., Barbosa-Morais, N.L., Schmidt, D., Conboy, C.M., Vanes, L., Tybulewicz, V.L., Fisher, E.M., Tavaré, S., and Odom, D.T. (2008). Species-specific transcription in mice carrying human chromosome 21. Science *322*, 434–438.

Yu, J., Yu, J., Mani, R.S., Cao, Q., Brenner, C.J., Cao, X., Wang, X., Wu, L., Li, J., Hu, M., et al. (2010). An integrated network of androgen receptor, polycomb, and TMPRSS2-ERG gene fusions in prostate cancer progression. Cancer Cell *17*, 443–454.

Yu, Y.P., Landsittel, D., Jing, L., Nelson, J., Ren, B., Liu, L., McDonald, C., Thomas, R., Dhir, R., Finkelstein, S., et al. (2004). Gene expression alterations in prostate cancer predicting tumor aggression and preceding development of malignancy. J. Clin. Oncol. *22*, 2790–2799.